DOI: 10.1002/minf.201400120

Design of Novel *Mycobacterium tuberculosis* Pantothenate Synthetase Inhibitors: Virtual Screening, Synthesis and In Vitro Biological Activities

Parthiban Brindha Devi,[a] Sridhar Jogula,[a] Asireddy Parameshwar Reddy,[a] Shalini Saxena,[a] Jonnalagadda Padma Sridevi,[a] Dharmarajan Sriram,[a] and Perumal Yogeeswari*[a]

Abstract: Pantothenate synthetase (PS) enzyme involved in the pantothenate biosynthetic pathway is essential for the virulence and persistent growth of *Mycobacterium tuberculosis* (MTB). It is encoded by the panC gene, and has become an appropriate target for developing new therapeutics for tuberculosis. Here we report new inhibitors active against MTB PS developed using energy based pharmacophore modelling of the available protein–inhibitor complex (3IVX) and virtual screening of a large commercial library. The e-pharmacophore model consisted of a ring aromatic (R), negative ionizable (N) and acceptor (A) sites. Compounds **5** and **10** emerged as promising hits with IC_{50}s 2.18 μM and 6.63 μM respectively. Further structural optimization was attempted to optimize lead **10** using medicinal chemistry approach and six compounds were found to exhibit better enzyme inhibition compared to parent compound lead **10** (< 6 μM).

Keywords: Pantothenate synthetase · e-Pharmacophore · Virtual screening · Enzyme ïnhibition · Hit optimisation · Tuberculosis

1 Introduction

Tuberculosis (TB), caused by *Mycobacterium tuberculosis* (Mtb), is an airborne infectious disease that affects almost one-third of the world's human population. Effective chemotherapy for TB has existed since the 1940s[1] however, an important factor contributing to the resurgence of the disease is due to emergence of multidrug resistant tuberculosis (MDR- TB). MDR-TB resistant atleast to the two most potent anti-TB drugs (isoniazid and rifampicin), affects nearly 630 000 people and incidence is on an increase in many parts of the world. Treatment of MDR-TB is complicated, and requires intense chemotherapy, continuous monitoring and seem to be very expensive. Recently, food and drug administration (FDA) has approved bedaquiline (sirturo), a diarylquinoline to treat MDR-TB.[2,3] Hence there seems to be an urgent need for new TB drugs that could shorten treatment regimen and could control drug resistant forms to be used along with the current AIDS/HIV retroviral treatments.

Pathogenicity associated with Mtb is mainly attributed to its lipid-rich cell wall which renders major challenge for the delivery of anti-mycobacterial agents. The cell wall synthetic pathway consisting of large number of genes encoding many enzymes have been found to be important for new drug discovery.[4] Among them, pantothenate synthetase (PS) encoded by panC gene useful in the production of pantothenate in bacteria, is the key precursor for the biosynthesis of coenzyme A (CoA) and acyl carrier protein (ACP), which in turn are important for fatty acid biosynthesis, cell signalling and biosynthesis of polyketides and non-ribosomal peptides.[5] It has been reported that an auxotrophic mutant of Mtb defective in the de novo biosynthesis of pantothenate was highly attenuated both in immunocompromised mice and in immunocompetent mice. This indicated that functional pantothenate biosynthetic pathway is very essential for the virulence of Mtb.[6] Moreover, PS is absent in mammals, as pantothenate is scavenged from diet through pantothenate permease and thus PS seem to be a potential target for the development of drugs against Mtb.

Recently, efforts toward discovery of Mtb PS inhibitors based on in-silico screening, synthetic modification and fragment based screening techniques were reported.[7–8] In continuation to our earlier reports and studies from our laboratory on Mtb PS inhibitors[9–12], we attempted an energy-based pharmacophore (e-pharmacophore) based on a reported crystal structure of Mtb PS-inhibitor complex and utilized it for a high-throughput virtual screening strat-

[a] *P. B. Devi, S. Jogula, A. P. Reddy, S. Saxena, J. P. Sridevi, D. Sriram, P. Yogeeswari*
Centre for Infectious Diseases Research, Birla Institute of Technology & Science-Pilani
Hyderabad Campus, Shameerpet, Hyderabad-500078, India
phone: +9140-66303515; fax: +9140-66303998
**e-mail: pyogee@hyderabad.bits-pilani.ac.in*

Supporting Information for this article is available on the WWW under www.molinf.com.

egy. On the basis of the e-pharmacophore model, followed by molecular docking and application of filtering criteria relevant to their important interactions with Mtb PS protein, 14 compounds were finally short-listed and further evaluated for in vitro Mtb PS inhibitory assay. Further synthetic modification was undertaken to derivatize a potential lead in order to get improved inhibitors for Mtb PS as a step towards lead optimization.

2 Experimental Procedures

2.1 Computational Details

All computations were carried out in an Intel Core 2 Duo E7400 2.80 GHz capacity processor with memory of 2 GB RAM running with the RHEL 5.2 operating system. PHASE 3.3 implemented with Maestro 9.3 software package (Schrodinger, LLC) was used to generate pharmacophore.[13] The virtual screening options for HTVS (High Throughput Virtual Screening), SP (Standard Precision) and Glide XP (extra precision) docking were all checked to be executed. Glide XP (extra precision) module of Schrödinger 9.3 (Glide, version 5.7, Schrödinger, LLC, New York, NY, 81 2011) was utilised for docking. The structure of MTB PS co-crystallized with {2-[(1-benzofuran-2-yl-sulfonyl)carbamoyl]-5-methoxy-1*H*-indol-1-yl}acetic acid [PDB: 3IVX] with resolution of 1.73 Å was retrieved from the protein data bank (www.rcsb.org).[14] Bond orders and formal charges were added to the hetero groups and hydrogen atoms were added to all atoms in the system.

2.2 Protein Preparation

Using protein preparation wizard and energy minimization the protein file was prepared. The wizard performed 500 cycles of steepest descent (SD) and 5000 cycles of conjugate gradient (CG) methods with optimized potential for liquid simulations (OPLS) 2005 force field using Schrodinger suite version 9.3. The active site of the protein was located and grid files were generated using receptor grid generation panel. The "Write XP descriptor information" option was selected and "Compute RMSD" option was enabled and rest of the parameters were kept as default. The XP Glide scoring function was used to order the best ranked compounds and the important interactions like π-cation and π–π stacking were analyzed using XP visualizer in Glide module. The input RMSD of the crystal ligand was also ascertained.

2.3 Development of e-Pharmacophore Models

Pharmacophore sites were automatically generated with PHASE (Phase, v3.0, Schrodinger, LLC, New York, NY) to the refined crystal ligand.[15] For the generation of e-pharmacophore, docking post-processing module of script option was selected and input file was in .xpdes format.[16] The default set of ten chemical features: hydrogen bond acceptor (A), hydrogen bond donor (D), hydrophobe (H), negative ionisable (N), positive ionisable (P) and aromatic ring (R) was used to derive the important pharmacophore features. Hydrogen bond acceptor sites were represented as vectors along the hydrogen bond axis in accordance with the hybridization of the acceptor atom. Hydrogen bond donors were represented as projected points, located at the corresponding hydrogen bond acceptor positions in the binding site. Projected points allowed the possibility for structurally dissimilar active compounds to form hydrogen bonds to the same location, regardless of their point of origin and directionality. Each pharmacophore feature site was first assigned an energetic value equal to the sum of the Glide XP contributions of the atoms comprising the site, allowing sites to be quantified and ranked on the basis of the energetic terms.[17]

2.4 Energy-Based Pharmacophore Validation

For validating the best of pharmacophore hypotheses, enrichment calculation was performed using a decoy set consisting of 1000 molecules with molecular weight ranging from 400–500 kDa along with 29 active molecules of Mtb PS inhibitors. E-Pharmacophore validation was used to check the hypothesis to discriminate the active Mtb PS compounds from the inactive molecules. Enrichment factor (EF), goodness of fit (GH), % actives, and % yield were calculated using the following equations.[18]

$$EF = \frac{(H_a \times D)}{(H_t \times A)} \quad (1)$$

$$GH = \left(\left(\frac{H_a}{4H_tA}\right) \times (3A + H_t)\right) \times \left(1 - \left(\frac{H_t - H_a}{D - A}\right)\right) \quad (2)$$

$$\%Yield = \left[\left(\frac{H_a}{H_t}\right) \times 100\right] \quad (3)$$

$$\%A = \left[\left(\frac{H_a}{A}\right) \times 100\right] \quad (4)$$

Where H_t represents the total number of compounds in the hit list, H_a the total number of active molecules in the hit list, A the total number of actives in the decoy set, and D the total number of molecules in the decoy set.

2.5 Preparation of Database

The commercial database Asinex (www.asinex.com) with 500 000 molecules were processed through redundancy check and Lipinski filter to select compounds with better drug-like property. All the structures were prepared using LigPrep (LigPrep v2.2, Schrodinger LLC, New York, NY) and Epik (Epik v1.6, Schrodinger, LLC, New York, NY) to expand protonation and tautomeric states at 7.0 ± 2.0 pH units.[14]

Conformational sampling was also performed for all the molecules using the ConfGen search algorithm. Confgen with OPLS 2005 force field was applied for generation of conformers and those duplicate poses were eliminated with RMSD less than 2.0 Å. A distance dependent dielectric constant of 4 and maximum relative energy difference of 10 kcal mol^{-1} were applied. Using Phase, the database was indexed with automatic creation of pharmacophore sites for each conformer to allow rapid database alignments and screening.

2.6 Molecular Docking

The best predicted and validated pharmacophore was subjected to screen compound libraries from Asinex. Virtual screening of the compound library was carried out by using Glide module of Schrodinger, LLC, 2012. Primarily, by using Glide module, we examined for favourable interactions between screened ligand hits (from pharmacophore screening) and the PS in the flexible mode docking. Three modes of Glide were available, high-throughput virtual screening (HTVS), standard precision (SP), and extra precision (XP) mode to be utilized in our protocol. The XP mode was used for exhaustive sampling and advanced scoring, resulting in higher enrichment. In the present study, we used Glide XP score for finding the best conformer with optimum binding affinity. The best conformer of each of the compounds along with the binding pose was given as input for e-pharmacophore mapping.[19–20]

2.7 Biological Assessments

2.7.1 Protein Expression

The Mtb panC gene (Rv3602c) encoding PS was cloned and transformed into BL21 (DE3) cells. Transformants were grown in LB broth at 37 °C with constant aeration, in the presence of 50 μg/mL kanamycin. Exponentially growing cultures (A600 of ~0.6) were induced with 0.8 mM IPTG (Isopropyl β- D-1-thiogalactopyranoside) and further grown for 12–16 h at 24 °C. Cells were harvested and lysed by sonication in lysis buffer containing 20 mM HEPES, pH 7.8, 500 mM NaCl, and 0.5 mM PMSF (phenylmethanesulfonyl fluoride). The cell lysate containing His 6-fusion proteins were equilibrated with Ni-NTA affinity resins and the tagged proteins were eluted with buffer containing 250 mM imidazole. The fractions containing PS protein were pooled for further enzymatic studies.

2.7.2 Mtb PS Screening

To each well of a 96-well plate, 60 μL of PS reaction mixture consisting of 0.4 mM NADH, 5 mM pantoic acid, 10 mM $MgCl_2$, 5 mM β-alanine, 10 mM ATP, 1 mM potassium phosphoenolpyruvate, and 20 μL of enzyme mixture (18 units/mL each of chicken muscle myokinase, rabbit muscle pyruvate kinase, and rabbit muscle lactate dehydrogenase) were taken. Both the reaction and enzyme mixtures were added to the plate to a final volume of 100 μL with 100 mM HEPES buffer (pH 7.8). Compounds were added to plates and the reaction was initiated with the addition of 10 μL of 4.32 pM of Mtb PS, diluted in buffer. The test plate was immediately transferred to a microplate reader and the depletion of NADH was measured at 340 nm. The reaction components except Mtb PS were mixed in the well and the background reaction was measured; Mtb PS was then added and the reaction kinetics was monitored.[21] The same method was followed for testing the designed inhibitors with different concentration. Reactions were carried out at 37 °C in a heat-controlled Perkin Elmer Victor V3 Spectrophotometer. % Inhibition were calculated using following formula

$$\%\,\text{Inhibition} = 100 \times \left\{\frac{1-\text{compound rate-background rate}}{\text{Full reaction rate-background rate}}\right\}$$

In order to confirm the specific inhibition of Mtb PS, coupled enzyme assay was performed in which the final concentration of lactate dehydrogenase was 0.2 units/mL and no substrate (pantoate) was added. The assay was then initiated with 6.5 mM of AMP instead of Mtb PS.

2.7.3 In Vitro Antimycobacterial Screening

The compounds were further screened for their in vitro antimycobacterial activity against *M. tuberculosis* H37Rv by microplate alamar blue assay method.[22] The inoculum was prepared and resuspended in 7H9 medium [7H9 broth, 0.1% casitone, 0.5% glycerol, supplemented 10% OADC (oleic acid, albumin, dextrose, and catalase)], and diluted to 1:20; 100 μL was used as inoculum. The drug concentration was diluted in 7H9 media and it was serially diluted. The growth control without antibiotic and sterile control were also kept on 96 well microtiter plates. Isoniazid and ethambutol were kept as positive controls. Sterile water was added to all surface wells in order to avoid evaporation during incubation. The plate was incubated for 7 days at 37 °C in normal atmosphere. After incubation, 1:1 of alamar blue and 10% tween solution were added to each wells, and the plate was reincubated for 3–4 h. A change in colour from blue (oxidised state) to pink (reduced) indicated the growth of bacteria, and the MIC was defined as the lowest concentration of drug that prevented this change in colour.

2.7.4 In Vitro Cytotoxicity Screening

The designed and synthesized compounds that showed good in vitro activity against PS assay were further examined for cytotoxicity using human embryonic kidney cells (HEK 293) at a single concentration of 50 μM.[23] HEK 293 cells were normal human embryonic cells widely used

for drug toxicity studies. HEK 293 cells were seeded in 96-well plates at an initial concentration of 5000 cells per well. After 24 h of incubation, the test compounds were added to the cells. After 48 h of exposure, viability of cells was assessed on the basis of conversion from 3-(4,5-dimethylthiazol-2-yl)-2,5 diphenyltetrazolium bromide (MTT) into formazon crystals.[24] Absorbance was then read on Perkin Elmer victor X3 plate reader at a wavelength of 595 nm. Relative to the control wells, the % growth was calculated for each well. The percentage of cells killed was obtained from the formula.

$$\text{Percentage of cells killed} = \frac{(100 - \text{mean OD sample})}{(\text{Mean OD day 0})}$$

2.7.5 Differential Scanning Fluorimetry (DSF)

The active compounds from this series of chemical class of molecules were further investigated using differential scanning fluorimetry.[25] The ability of the compounds to stabilize the Mtb PS protein was assessed utilizing DSF technique by which the thermal stability of the Mtb PS native protein and the protein with ligands were measured. Briefly, the native protein PS (7 μL of protein (0.23 mg/mL) + 9 μL of assay buffer (100 mM HEPES-NaOH, pH-7.8)) was subjected to stepwise heating in a real time PCR instrument (Bio-Rad iCycler5) from 25 to 95 °C in steps of 0.1 °C rise in the presence of a fluorescent dye SYPRO orange (Sigma), whose fluorescence increased as it interacted with protein. As the proteins get denatured the hydrophobic residues became exposed to the dye. A right side positive shift of T_m in comparison to native protein meant higher stabilization of the protein-ligand complexes, which was a consequence of the inhibitor binding.

2.8 Synthetic Chemistry

2.8.1 Preparation of Methyl D-tryptophanate (2)

To a solution of thionyl chloride (4.25 mL, 58 mmol) in methanol (50 mL) was added D-tryptophan (5 g, 24.5 mmol) and the resulting solution was heated under reflux for 18 h. After evaporation of the solvent, a white residue of hydrochloride salt was obtained, which was neutralized by a sodium carbonate solution and the ester was extracted with ethyl acetate (200 mL). The organic layer was dried over sodium sulfate and evaporated under reduced pressure to obtain 5 g (yield 93%) of compound as off-white solid.

1 H NMR (δ, ppm, DMSO-d_6, 300 MHz): 3.39 (m, 2 H), 3.63 (s, 3 H), 4.20 (t, 1 H, J = 5.5), 7.07 (dt, 2 H, J = 21), 7.26 (d, 1 H, J = 3), 7.39 (d, 1 H, J = 7.8), 7.53 (d, 1 H, J = 7.8). ^{13}C NMR (DMSO-d_6, 100 MHz); 26.01, 52.61, 106.26, 111.45, 117.84, 118.50, 121.05, 124.80, 126.79, 136.13, 169.57; *m/z* 218 $[M+H]^+$.

2.8.2 Preparation of Methyl 2-(3-aminobenzamido)-3-(1H-indol-3-yl)propanoate (3)

To a stirred solution of **2** (5.00 g, 22.9 mmol) and 3-aminobenzoic acid (3.45 g, 25.22 mmol) in DMF (80 mL) was added DIPEA (7.38 g, 57.25 mmol) followed by O-(benzotriazol-1-yl)-N,N,N′,N′-tetramethyluronium tetrafluoroborate (8.82 g, 27.48 mmol). Then the reaction mixture was allowed to stir at room temperature for 16 h. The reaction mixture was diluted with water (50 mL) and extracted with EtOAc (100 mL); organic layer washed with water dried over sodium sulfate and evaporated under reduced pressure to obtain crude compound. This was purified by column chromatography to afford 5.10 g (yield 65%) of compound **3** as off-white solid.

^{1}H NMR (300 MHz, $CDCl_3$) δ:8.136 (bs, 1 H), 7.563 (d, *J* = 7.5 Hz, 1 H), 7.350 (d, *J* = 8.1 Hz, 1 H), 7.180–7.010 (m, 5 H), 6.663–6.531 (m, 3 H), 5.498 (bs, 2 H), 5.090–5.069 (m, 1 H), 3.713 (s, 3 H), 3.426 (d, *J* = 4.8 Hz, 2 H); MS (ESI) *m/z* 338 $[M+H]^+$.

2.8.3 General Procedure for Preparation of Compounds 4 (a–p)

To a stirred solution of compound **3** (1.00 equiv) in CH_2Cl_2 (10 vol) was added DIPEA (3.00 equiv) and cooled to 0 °C and slowly added corresponding acid chloride (1.30 equiv) and allowed to stir at room temperature for 12 h. Reaction mixture washed with water followed by 3N NaOH and brine; organic layer dried over sodium sulfate and evaporated under reduced pressure to obtain crude compound. This was purified by trituration with diisopropylether to afford **4(a–p)** respectively.

2.8.3.1 Methyl-3-(1H-indol-3-yl)-2-(3-(pyrazine-2-carboxamido)benzamido)propanoate (4a)

Yield: 65%; MS(ESI) *m/z* 444 $[M+H]^+$. ^{1}H NMR (400 MHz, $CDCl_3$) δ:12.07 (s, 1 H), 9.87 (s, 1 H), 9.29(d, *J* = 8.0, 1 H), 8.80(d, *J* = 8.2, 1 H), 8.08(bs, 1 H), 8.05–8.01(m, 2 H), 7.64–7.59 (m, 1 H), 7.33–7.29 (m, 1 H), 7.27 (t, *J* = 7.2, 1 H), 7.20–7.15 (m, 3 H), 7.07–6.95 (m, 1 H), 6.79 (d, *J* = 7.2, 1 H), 5.16–5.11(m, 1 H), 3.76 (s, 3 H), 3.49–3.41 (m, 2 H); ^{13}C NMR (100 MHz, $CDCl_3$) δ: 172.5, 168.6, 163.1, 149.9, 145.46, 143.9, 142.6, 129.5, 128.4, 127.0, 123.5, 122.8, 120.9, 120.1, 119.8, 118.3, 118.0, 116.0, 115.8, 112.4, 111.2, 54.54, 52.31, 29.4.

2.8.4 General Procedure for the Synthesis of Compounds 5 (a–p)

To a stirred solution of compound **4(a–p)** (1.00 equiv) in methanol (8 vol) was added 3N NaOH (3.00 equiv) and stirred at room temperature for 4 h. Evaporated the methanol and diluted with water, washed the aqueous layer with EtOAc. Adjusted the aqueous layer pH to 2 by using conc.

HCl and extracted with CH_2Cl_2 and concentrated and dried to afford the compounds **5 (a–p)** respectively.

The spectral data of representative compounds are given below.

2.8.4.1 2-(3-(4-Fluorobenzamido)benzamido)-3-(1H-indol-3-yl)propanoic acid (5e):

Yield: 92%; MS(ESI) *m/z* 444 $[M-H]^+$. ^{1}H NMR (400 MHz, DMSO-d_6) δ:12.2 (s, 1 H), 10.8 (s, 1 H), 9.07(d, J=8, 1 H), 8.59 (d, J=8, 1 H), 7.90–7.83 (m, 3 H), 7.61–7.55 (m, 2 H), 7.39 (t, , J=8, 2 H), 7.29 (d, J=8, 1 H), 7.20 (t, J=8, 2 H), 7.04 (t, J=8, 1 H), 6.96 (t, J=8, 1 H), 4.69–4.78 (m, 1 H), 3.43–3.21 (m, 2 H); ^{13}C NMR (100 MHz, DMSO-d_6) δ: 172.9, 168.7, 163.3, 139.2, 136.0, 132.46, 130.9, 129.6, 129.5, 128.4, 127.0, 123.5, 122.8, 120.9, 120.1, 119.8, 118.3, 118.0, 116.0, 115.8, 111.4, 110.2, 53.74, 26.42(2C).

2.8.4.2 2-(3-(4-Chlorobenzamido)benzamido)-3-(1H-indol-3-yl)propanoic acid (5h):

Yield: 89%; MS(ESI) *m/z* 460 $[M-H]^+$. ^{1}H NMR (400 MHz, DMSO-d_6) δ: 12.9 (bs, 1 H), 12.2 (s, 1 H), 10.803 (s, 1 H), 9.07 (d, J=8.0, 1 H), 8.58 (d, J=7.6, 1 H), 7.85–7.81 (m, 3 H), 7.646–7.550 (m, 4 H), 7.29 (d, J=15.6, 1 H), 7.230–7.189 (m, 2 H), 7.03 (t, J=6.0, 1 H), 6.96 (t, J=7.2, 1 H), 4.68–4.78 (m, 1 H), 3.33–3.25 (m, 2 H); ^{13}C NMR (100 MHz, DMSO-d_6) δ: 172.96, 168.71, 163.31, 139, 137.7, 136.8, 136.0, 133.1, 132.4, 131.1, 129.0, 128.7, 128.4, 127.0, 123.5, 122.9, 120.9, 119.9, 118.3, 118.0, 111.4, 110.2, 53.73, 26.80, 26.42.

2.8.4.3 2-(2-(4-tert-Butylbenzamido)benzamido)-3-(1H-indol-3-yl)propanoic acid (5p):

Yield: 75% ^{1}H NMR (400 MHz, $CDCl_3$) δ:11.945 (s, 1 H), 8.729 (d, J=8.4 Hz, 1 H), 8.181 (bs, 1 H), 7.989–7.925 (m, 1 H), 7.561–7.409 (m, 4 H), 7.253–7.187 (m, 2 H), 7.127 (t, J=7.2 Hz, 1 H), 7.026 (t, J=7.6 Hz, 1 H), 6.912–6.804 (m, 4 H), 5.131–5.099 (m, 1 H), 3.478–3.387 (m, 2 H), 1.255 (s, 9 H) ;^{13}C NMR (100 MHz,$CDCl_3$) δ: 175.35, 168.95, 165.93, 155.56, 139.95, 136.11, 133.01, 131.79, 130.14, 127.56, 126.97, 125.54, 123.10, 122.37, 121.65, 119.86, 118.48, 111.43, 109.44, 53.39, 35.00, 31.15; MS (ESI) *m/z* 482 $[M-H]^+$.

2.8.4.4 2-(2-Benzamidobenzamido)-3-(1H-indol-3-yl)propanoic acid (5n):

Yield: 70% ^{1}H NMR (400 MHz, DMSO-d_6) δ:12.251 (s, 1 H), 10.831 (s, 1 H), 9.090 (d, J=6.8 Hz, 1 H), 8.667 (d, J=8, 1 H), 7.871 (d, J=6.4, 2 H), 7.644–7.569 (m, 6 H), 7.337–7.193 (m, 3 H), 7.086–6.998 (m, 2 H), 4.764 (s, 1 H), 3.406–3.295 (m, 2 H); ^{13}C NMR (100 MHz, DMSO-d_6) δ: 173.02, 168.80, 164.38, 139.33, 136.11, 132.46, 128.93, 128.52, 128.45, 1 27.09, 126.86, 123.59, 122.70, 120.95, 120.13, 119.79, 118.37, 118.08, 111.44, 110.26, 53.77, 27.33; MS (ESI) *m/z* 426 $[M-H]^+$.

2.8.4.5 2-(2-(2-Fluorobenzamido)benzamido)-3-(1H-indol-3-yl)propanoic acid (5o):

Yield: 65% ^{1}H NMR (400 MHz, DMSO-d_6) δ:11.830 (s, 1 H), 10.809 (s, 1 H), 8.978 (d, J=7.6 Hz ,1 H), 8.578 (d, J=8.4 Hz, 1 H), 7.864–7.763 (m, 2 H), 7.656–7.545 (m, 3 H), 7.399–7.342 (m, 3 H), 7.319–7.299 (m, 2 H), 7.047 (t, J=7.2 Hz, 1 H), 6.965 (t, J=7.2 Hz, 1 H), 4.697–4.643 (m, 1 H), 3.363–3.209 (m, 2 H); ^{13}C NMR (100 MHz, DMSO-d_6) δ: 173.02, 168.23, 161.41, 160.53, 158.05, 138.49, 136.09, 133.83, 133.74, 132.16, 130.59, 128.38, 127.10, 125.01, 124.98, 123.51, 122.87, 122.74, 120.91, 120.85, 120.79, 118.32, 118.06, 116.69, 116.49, 111.39, 110.25, 53.68, 26.41; MS (ESI) *m/z* 444 $[M-H]^+$.

3 Results and Discussions

The major aim of our drug design efforts was to identify and develop new ligands with high affinity of binding towards the target protein. A very useful model employed for achieving this aim was structure-based design. It was a prerequisite to have accurate starting structures which could enhance the chances of retrieving similarly active and diverse hits from database screening. In the present study crystal structure of the Mtb PS protein co-crystallized with inhibitor [PDB: 3IVX] retrieved from the protein data bank (www.rcsb.org) was utilised as a structural framework for virtual screening to discover newer class of PS inhibitors. HTVS (High Throughput Virtual Screening); SP (Standard Precision) and Glide XP (extra precision) docking options for virtual screening were used. Glide XP (extra precision) module of Schrödinger 9.2 (Glide, version 5.7, Schrödinger, LLC, New York, NY, 2011) was finally utilised for docking as it combined accurate, well defined physics-based scoring terms and thorough sampling of the database ligands.

3.1 Protein Preparation and Active site Validation

The retrieved protein was prepared using protein preparation wizard by adding hydrogen atoms, removed water molecules and energy minimization by converging the heavy atoms using OPLS_2005 as force field. The orientations of the ligand in the active site pocket with the interactions between the ligand and protein atoms were visualized. To validate the method in predicting binding energy and possible interaction between ligands and receptor, at first existing ligand in the crystal structure was re-docked with the protein. The crystal ligand showed a docking score of -9.75 kcal mole^{-1} retaining important interactions with Val187, Ser196, Hie44 (protonated state of Histidine), Hie47, and Met40. Representation of crystal ligand in the active site of protein and its ligand interaction diagram are shown in Figures 1 A and 1 B. The root mean square deviation (*RMSD*) of re-docked ligand and original crystal ligand was found to be 1.13 A°. The superimposition of docked

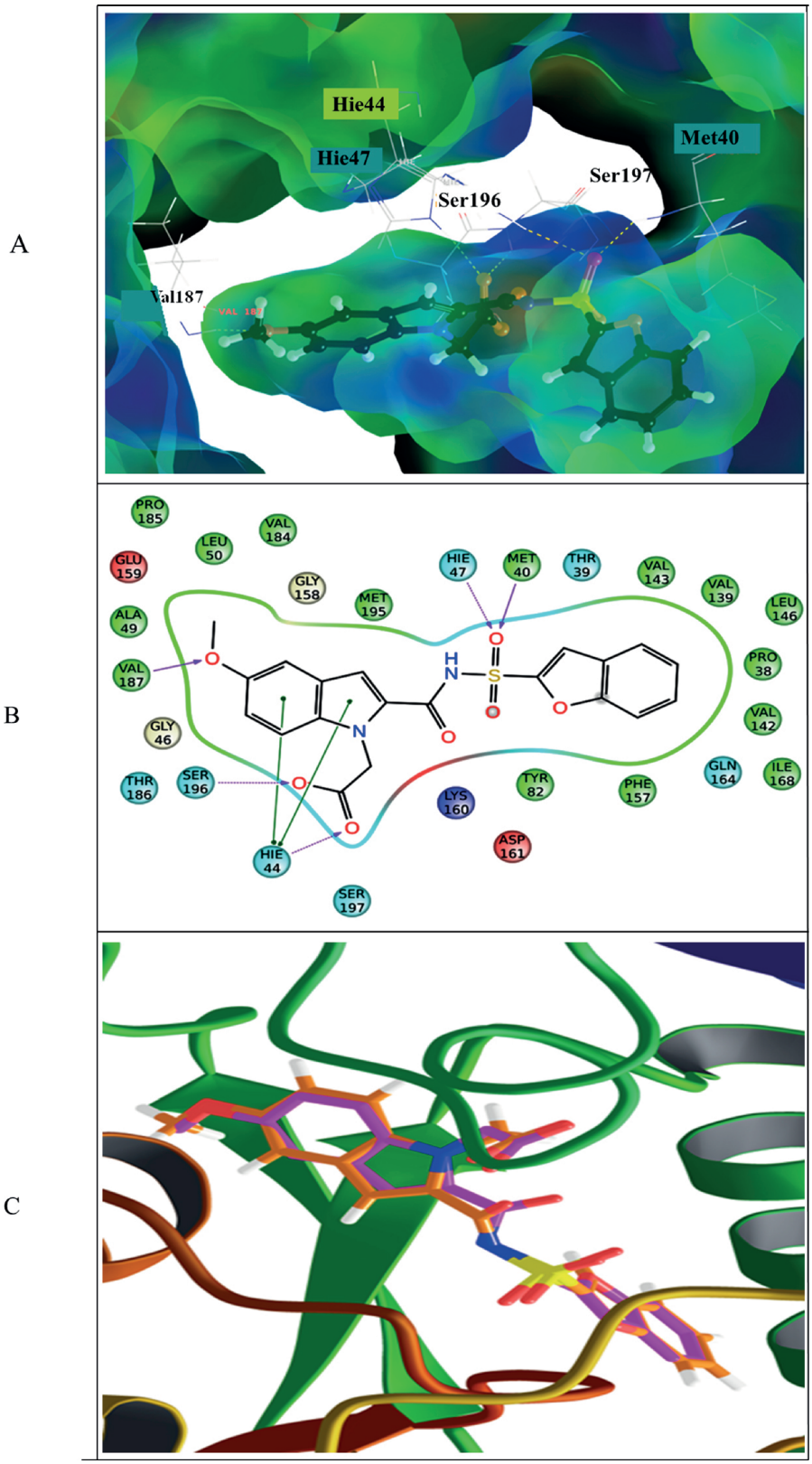

Figure 1. Binding pose (A) of crystal ligand towards protein active site and its ligand interaction diagram (B). Superimposition of crystal ligand along with the redocked ligand (C) where Pink represents the original pose of crystal ligand Orange represents the docked pose of crystal ligand.

pose and crystal ligand at the active site of the protein is depicted in Figure 1C.

3.2 E-Pharmacophore Generation

The e-pharmacophore method which combined the aspects of structure-based and ligand-based techniques was explored for the Mtb PS protein. The result of XP docking was used to determine the pharmacophoric features of the protein. The energy based pharmacophore hypotheses were developed by mapping Glide XP energetic terms onto pharmacophore sites. The initial number of pharmacophore sites was set up to 10 for the crystal structure. The results of the e-pharmacophore generation of the reference ligand were used to identify the best pharmacophore hypothesis. The energy score of the pharmacophoric features is represented in Table 1.

Table 1. E-Pharmacophore features.

Rank	Feature Label	Score	Interaction
1	N7	−0.76	Hbond
2	A4	−0.35	Hbond
3	R11	−1.14	Ringchemscore Hphobe
4	R12	−0.93	Ringchemscore Hphobe
5	R9	−0.56	Ringchemscore Hphobe

The energy contribution for binding of a ligand to the protein was the key to derive pharmacophoric features in structure-based design. The generated e-pharmacophores showed three aromatic rings required for the hydrophobic interaction within the pocket namely R9 (score −0.56), R11 (score −1.14) and other R12 (score −0.93) together with an acceptor site namely A having score −0.35 and one negative ionisable group with score of −0.76. On an average, there were 5 sites per hypothesis, many of which did not even appear to be directly involved in protein-ligand interactions. Based on energy score and distance between each pharmacophore point of the hypothesis we made a combination of pharmacophores having 5, 4 and 3 point features that yielded a total of 6 hypotheses.

3.3 E-Pharmacophore Validation

The six e-pharmacophore hypotheses were subjected for validation using decoy set containing 1000 compounds along with 29 known Mtb PS inhibitors (http://www.brenda-enzymes.info/). Ligand decoy sets were available for download as provided by Schrodinger (http://www.schrodinger.com/glide_decoy_set). Hypothesis 2, a four point model (RRRN) containing three aromatic rings (R) and one negative ionizable group (N) displayed good enrichment factor (EF), goodness of fit (GH) and satisfied all other validation parameters of a true pharmacophore model (Table 2). Similarly, hypothesis 5, a three point model (RRA) containing two aromatic rings (R) and one hydrogen acceptor (A) also yielded better parameters of a true pharmacophore model. From the overall validations, we concluded that hypothesis 2 (RRRN) and hypothesis 5 (RRA) could predict most of the experimentally active molecules than the remaining four hypotheses that were compared. The results are as shown in Table 2, where hypothesis 2, 5 and 6 showed good enrichment at 1% (EF1%) and Goodness of hit values compared with other hypothesis.

Thus the four point (Hypothesis 2) and three point (Hypothesis 6) e-pharmacophore models were used for the virtual screening of commercial database (Asinex). The selected e-pharmacophores are shown in Figure 2.

3.4 Virtual Screening of Molecules

Virtual screening was of cardinal importance in in-silico drug discovery process to speed up drug development, as it helps in the selection of the best candidate drugs. The virtual screening protocol reported in this study was based on the application of sequential filters to select restricted number of compounds. The validated e-pharmacophore models were used in turn to screen the compounds from Asinex database. Fit values represented how effectively the ligand could fit to the e-pharmacophore model. In this study, the hits retrieved by two e-pharmacophore models with fit values above 1.0 were carried forward to HTVS. Top hits from HTVS with docking score of ≤ -6.0 kcal mol^{-1} were subjected to docking using Glide XP. The results of the virtually screened ligands using Glide XP helped to find accurately the hydrogen-bond interactions, electrostatic interaction, hydrophobic interactions and π–π stacking inter-

Table 2. E-pharmacophore hypothesis and its validation.

Hypothesis	E-pharm features	*EF* [a]	GH [b]	% Yield [c]	% A [d]
1	5features (R12,R9,R11,A4,N7)	0.91	0.04738	2.505	82.14
2	4features (R12,R9,R11,N7)	1.88	0.1399	5.14	78.57
3	4features (R12,R9,R11,A4)	0.954	0.037	2.6	78.5
4	3features (R12,R11,N7)	0.63	0.02	1.724	3.448
5	3features (R12,R11,A4)	1.69	0.107	4.624	57.724
6	3features (R12,R11,R9)	1.86	0.047	5.06	53.57

[a] Enrichment factor; [b] goodness of fit score; [c] % yield of actives; [d] ratio of actives.

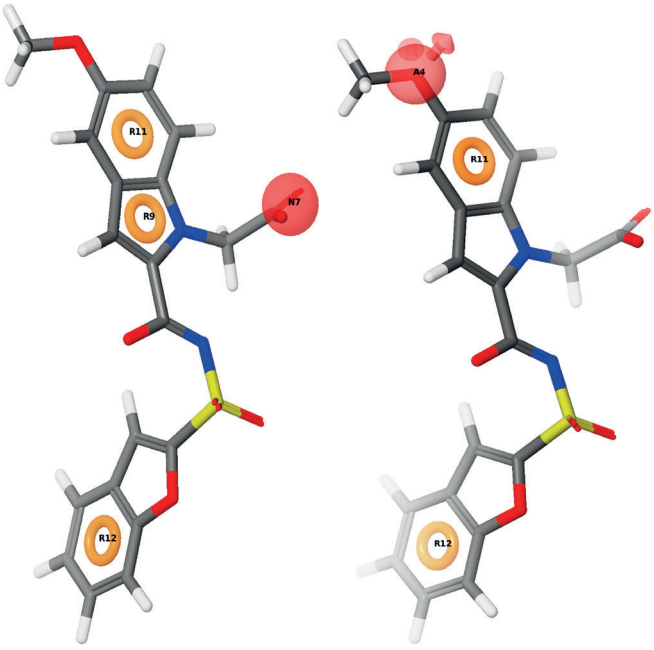

Figure 2. Energy based pharmacophore hypothesis selected for HTVS.

actions. The results showed that the docking score ranged from −7.471 to −10.523 kcal mol^{-1}. Further the hits from Glide XP were evaluated using GOLD 4.1.2 (genetic algorithm based docking) to confirm the interactions of leads in the active site of the protein. The GOLD scores of the selected hits were found to be in the range from 50.5 to 72.57. In addition to docking scores, final short listing of possible lead molecules were based on visual inspection of important interacting amino acids Val187, Ser196, Hie44, Hie47 and Met40 in the PS protein. We finally selected top fourteen compounds, whose docking score, hydrogen bonds and important interactions are represented in Table 3 and the structures are presented in Figure 3. The active site of the protein with these ligands were obtained using ligand interaction diagram in Schrodinger suite. The selected hits were found to be well placed in the active site of the protein. Further to prove the design concept, the final hits were procured from Asinex database, and subjected to Mtb PS enzyme inhibition study and biophysical assay using differential scanning fluorimetry to further check the binding affinity of the active ligand towards the protein.

3.5 Preliminary Biological Screening

The lead compounds were assayed for Mtb PS inhibition study; ATP-dependent catylsis with condensation of pantoate and ß-alanine to yield pantothenate, AMP and pyrophosphate. The formation of AMP from MTB PS catalysed reaction was coupled with the reactions through myokinase, pyruvate kinase and lactate dehydrogenase. The decrease in the absorbance of NADH was spectrophotometrically monitored at 340 nm. In the initial screening at 50 μM, all the compounds showed more than 50% inhibition against MTB PS and were further studied for IC_{50} measurements with varying concentrations 50 μM, 10 μM, 5 μM and 1 μM respectively. The results are presented as Table 4.

All the compounds inhibited MTB PS activity with IC_{50}s values ranging from 2.18–50 μM. The most active molecule from in-silico screening was found to be lead **5** with IC_{50} of 2.18 μM. Other promising hits included **4**, **7**, **10**, **11** and **14** that exhibited IC_{50}s less than 10 μM. Diagrammatic representation of potent molecule **5** binding mode and its ligand interaction is shown in Figure 4.

3.6 Lead Optimisation

Based on the preliminary screening of hits identified by the in-silico modelling, it was evident that e-pharmacophore hypothesis employed in the study was successful. To further our medicinal chemistry questin optimizing the lead, we attempted to structurally modify lead **10** to improve the potency and also derive a structure-activity relationship to understand better. Lead 10 was preferred due to similari-

Table 3. Docking parameters of the identified leads.

Compound ID	Fitness	Docking score	Hydrogen bond	Gold score	Ligand interaction
Lead 1	1.70	−10.11	6	65.99	Lys160, Ser197, Hie44, Met195
Lead 2	1.94	−10.07	8	51.53	Asp161, Gly158, Hie44, Ser197, Ser196, Val187, Gly46
Lead 3	1.67	−9.66	7	60.8	Ser197, Ser196, Hie44, Lys160, Met195
Lead 4	2.42	−10.81	7	72.35	Gln164, Ser197, Ser196, Pro38, Gly158, Val187
Lead 5	1.66	−10.69	8	73.10	Gln164, Pro38, Hie44, Lys160, Ser197, Asp161, Ser196
Lead 6	2.10	−10.27	6	60.73	Pro38, Val187, Gln164, Lys160, Arg198, Ser197
Lead 7	2.22	−10.19	7	74.31	Met40, Pro38, Asp161, Lys160, Hie44, Ser197, Gln72
Lead 8	2.08	−9.80	7	74.83	Gly158, Gln164, Gln72, Hie47, Ser196, Ser197, Asp161, Lys160
Lead 9	1.12	−8.71	5	69.25	Gln72, Ser197, Ser196, Hie44
Lead 10	1.59	−8.40	5	70.80	Hie44, Hie47, Ser197, Ser196, Lys160
Lead 11	1.82	−9.28	7	78.73	Lys160, Hie44, Ser197, Ser196, Val187
Lead 12	2.08	−9.13	5	69.1	Gln164, Asn161, Lys160, Hie44, Val187
Lead 13	2.15	−9.00	6	66.87	Ser196, Val187, Hie44, Hie47, Ser197, Met40
Lead 14	1.62	−12.84	7	68.85	Arg198, Gln164, Gly158, Ser197, Ser196, Asp161, Hie44

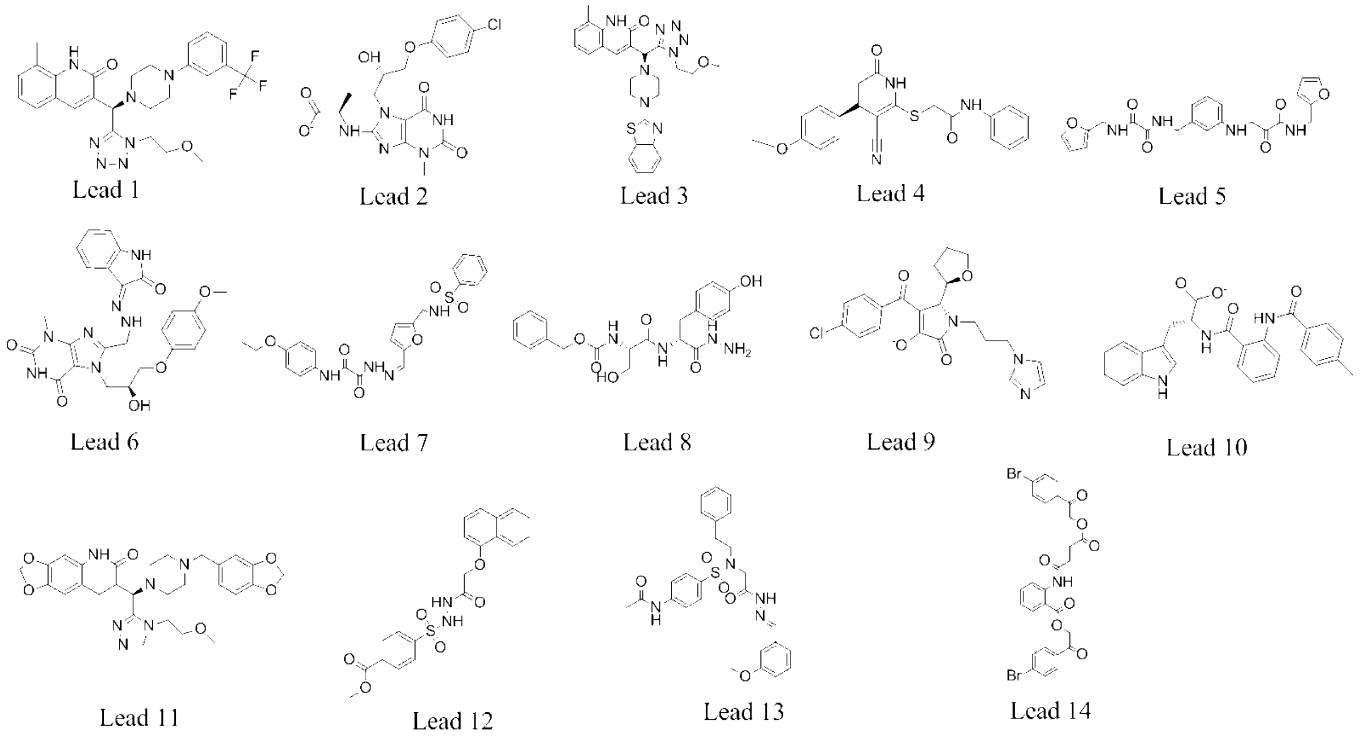

Figure 3. Structures of the final shortlist based on e-pharmacophore filtering, HTVS, GLIde SP and XP and GOLD docking.

Table 4. Biological assessments of designed compounds.

Compound ID	IC_{50} (μM) [a]	MTB MIC (μM) [b]	Cytotoxicity at 50 μM [c]
Lead 1	>50	47.390	29.50 ± 0.125
Lead 2	11.36	28.550	37.87 ± 0.264
Lead 3	10.77	24.196	47.44 ± 0.010
Lead 4	2.81	15.885	31.67 ± 0.0299
Lead 5	2.18	14.255	24.49 ± 0.039
Lead 6	>50	98.916	45.23 ± 0.011
Lead 7	4.04	53.136	32.49 ± 0.0749
Lead 8	14.98	30.018	55.49 ± 0.0218
Lead 9	16.5	15.176	60.83 ± 0.0129
Lead 10	6.63	56.629	28.73 ± 0.0218
Lead 11	4.27	22.834	54.201 ± 0.0911
Lead 12	>50	60.324	66.80 ± 0.0657
Lead 13	23.33	49.196	21.34 ± 0.1334
Lead 14	8.75	19.802	30.48 ± 0.0145
Isoniazid	ND	0.72	ND
Ethambutol	ND	7.64	ND

[a] MTB PS enzyme inhibitory assay; [b] minimum Inhibitory concentration against *M. tuberculosis* H37 Rv; % inhibition of HEK293 cells, where, ND represents Not Determined.

ty with the crystal ligand based on tanimotocombo similarity predicted to be in the range of 0.52–0.68 (Supporting information) and synthetic feasibility as we had earlier worked on indole nucleus. The target molecules were synthesised by following a four step synthetic scheme (Figure 5) starting with a commercially available, less expensive 2-amino-3-(1H-indol-3-yl)propanoic acid (**1**) (Scheme 1 in Figure 5). In the first step we protected the acid group of starting material with methyl group. Then the obtained methyl 2-amino-3-(1H-indol-3-yl)propanoate (**2**) was treated with 3-aminobenzoic acid, TBTU and DIPEA in N,N-dimethyl formamide to afford methyl 2-(3-aminobenzamido)-3-(1H-indol-3-yl)propanoate derivative (**3**).

We employed corresponding acid chlorides to synthesise compounds 4 (a–p), since the attempts to couple the carboxylic acid group with the amine using coupling agents (EDCI/HOBt and HATU) failed to obtain desired product. The purity of the synthesized compounds was checked by

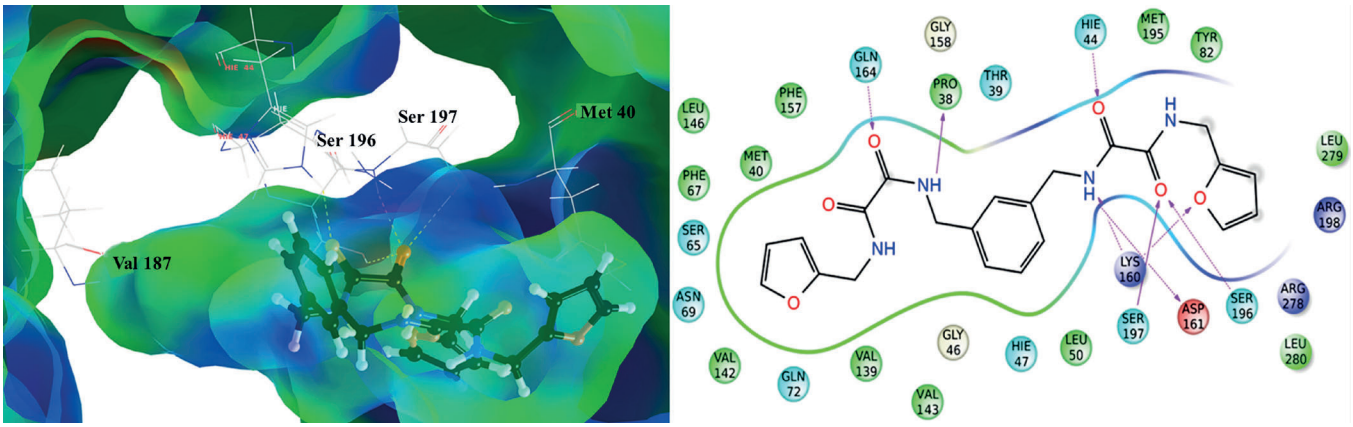

Figure 4. Binding pose of top active lead molecule (5, from asinex database) and its ligand interaction diagram towards the active site of the protein.

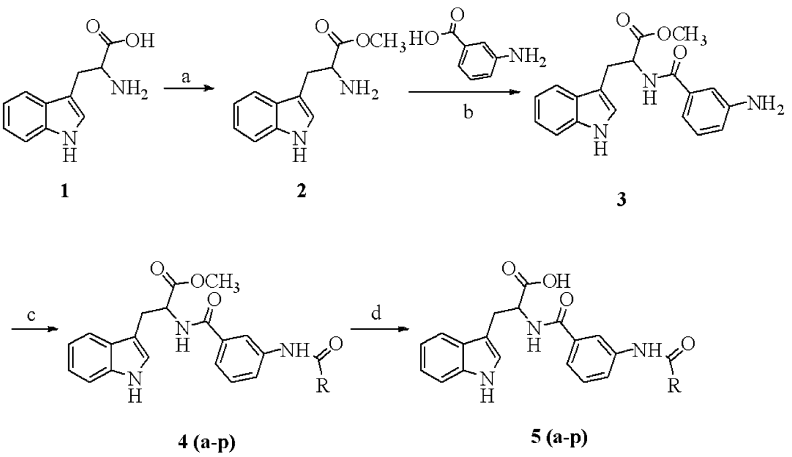

Reagents & Conditions: a: $SOCl_2$, MeOH, reflux, 18 h; b: TBTU, DIPEA, DMF, rt, 16 h; c: RCOCl, CH_2Cl_2, rt, 12 h; d: 3N NaOH, MeOH, rt, 4 h:

Figure 5. Synthetic protocol depicting the steps involved in the synthesis of lead 10 analogues.

LC–MS, the fstructures were confirmed by spectral data. In the nuclear magnetic resonance spectra (^{1}H NMR and ^{13}C NMR), the signals of the respective protons of the prepared derivatives were verified on the basis of their chemical shifts, multiplicities, and coupling constants.

3.7 In Vitro Enzymatic Assay

Further, the synthesized compounds (**5a–5p**) were evaluated for their in vitro enzymatic inhibition assay. As there were no reported inhibitors for Mtb PS till date we did not employ any positive control in the assay. The coupled assay was found to prove that compounds designed and synthesised were specific towards Mtb PS and were not active against enzymes used in the reaction. Further IC_{50} values and dose response curves were plotted against concentrations in logarithmic scale and % inhibition using Graphpad prism 5 software. The R-position was substituted with different aromatic residues in-order to maintain bulky and hydrophobicity. Among the synthesized compounds, about six compounds were found to be more active than the parent **lead 10** with IC_{50}s less than 6 μM. Compound **(5e)** with 4-fluorophenyl substitution was found to exhibit better activity when compared to the parent molecule with an IC_{50} of 2.287 ± 0.03 μM. Post lead optimization, compound **5e** emerged to be 3 times more potent than the parent molecule (**10**). The IC_{50}s of all 16 compounds in Mtb PS inhibition assay is represented in Table 5. The dose-response curve is represented in Figure 6.

Docking studies revealed that the parent molecule (**Lead 10**) was associated with five hydrogen bonds as shown in Table 3. The binding mode and ligand interaction diagrams of lead **10** along with compounds **5e** and **5l** are shown in Figure 7 A–C. Closer analysis of the docked ensembles with ligand showed key hydrogen bonding with His44, His47, Met40, Ser196, Ser197 and Val187. The hydrophobic pocket included Pro38, Met40, Thr39, Phe157 and Leu50 residues. The binding analysis of most active com-

Table 5. Biological assessment of synthesized molecules.

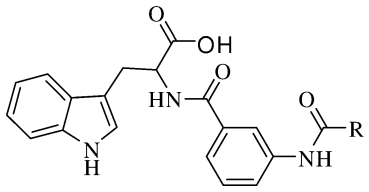

Compound ID	R	IC_{50} (μM) [a]	MIC (μM) [b]	Cytotoxicity (HEK293 cells) 50 μM [c]
5a	2-Pyrazine	10.68 ± 0.02	56.376	48.153 ± 0.0158
5b	Cyclohexyl	7.74 ± 0.04	55.862	25.194 ± 0.0225
5c	Cyclopentyl	7.14 ± 0.08	28.835	38.209 ± 0.0248
5d	2-Thiophene	9.30 ± 0.01	55.865	40.225 ± 0.0015
5e	4-Fluoro phenyl	2.28 ± 0.03	27.205	24.843 ± 0.0091
5f	4-Methoxybenzyl	15.63 ± 0.06	13.256	63.358 ± 0.0154
5g	2-Trifluoromethyl phenyl	8.52 ± 0.01	24.535	32.124 ± 0.0052
5h	4-Chlorophenyl	5.21 ± 0.02	52.530	22.692 ± 0.0119
5i	3-Chlorophenyl	10.87 ± 0.01	52.530	43.346 ± 0.0003
5j	2-Furoyl	6.82 ± 0.04	28.973	37.038 ± 0.0202
5k	2-Chlorophenyl	10.06 ± 0.06	52.530	53.592 ± 0.0188
5l	3-Nitrophenyl	2.88 ± 0.07	51.390	43.528 ± 0.0375
5m	4-Nitrophenyl	9.54 ± 0.04	102.779	32.210 ± 0.0580
5n	Phenyl	3.59 ± 0.06	28.314	39.860 ± 0.0613
5o	2-Fluoro	5.62 ± 0.01	54.411	56.295 ± 0.0434
5p	4-*tert*-butyl phenyl	4.45 ± 0.02	12.561	50.340 ± 0.0167

[a] MTB PS enzyme inhibitory assay; [b] minimum Inhibitory concentration against *M. tuberculosis* H37 Rv; [c] % inhibition of HEK293 cells.

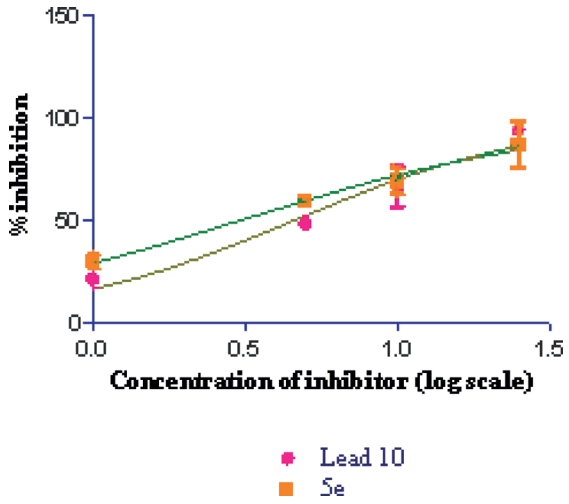

Figure 6. Dose response curve for the active molecules using Graphpad Prism software

pounds **5e** and **5l** in the active site of PS protein revealed that they possessed good docking scores (−9.24 and −8.86 kcal/mol) and formed hydrogen bonds with HIE44, Ser196, and Ser197 which were conserved with the reference ligand too. In compound **5e,** the 4-flourophenyl group at R position was found to be inserted into the hydrophobic pocket formed by the Pro38, Met40, Phe157, Ile166, Val139, Val142 and Val143 amino acid residues, while in compound **5l** the 3-nitrophenyl group at R position was positioned in the hydrophobic patch formed by Pro38, Met40, Phe67, Val142, Val143, and Val139 residues which exhibited strong hydrophobic interactions. The binding patterns within the active site pocket of both the active compounds and reference ligand were quite similar. A closer analysis of the interaction profile revealed that compounds **5e** and **5l** showed interactions with Gln72 and Asp161 which were missing with lead **10**.

3.8 Thermal Shift Assay (DSF)

Differential scanning fluorimetry (DSF) measured the thermal stability of a target protein when bound to a ligand. The binding of the potent ligand **5e** was evaluated by measuring the fluorescence of the native protein and protein-ligand complex in presence of a fluorescent dye whose fluorescence increased when exposed to non-polar residues of the protein and reached the maximum when the protein got denatured. Figure 8 represents the thermal shift binding assay of the molecule **5e**. The protein showed melting temperature (T_m) of 42.30 °C, whereas with molecule **5e** the corresponding melting temperature was found to be 44.30 °C. The difference in the melting temperature values showed how effectively the ligand stabilized the protein due to binding with the protein. Compound **5e** displayed a T_m shift of 2 °C which further was re-ascertained for their stabilization towards the Mtb PS protein which correlated with its PS IC_{50} of 2.287 μM.

3.9 In Vitro AntimyCobacterial and Cytotoxicity Screening

Further the designed and synthesized compounds were screened for their in vitro anti-mycobacterial activity

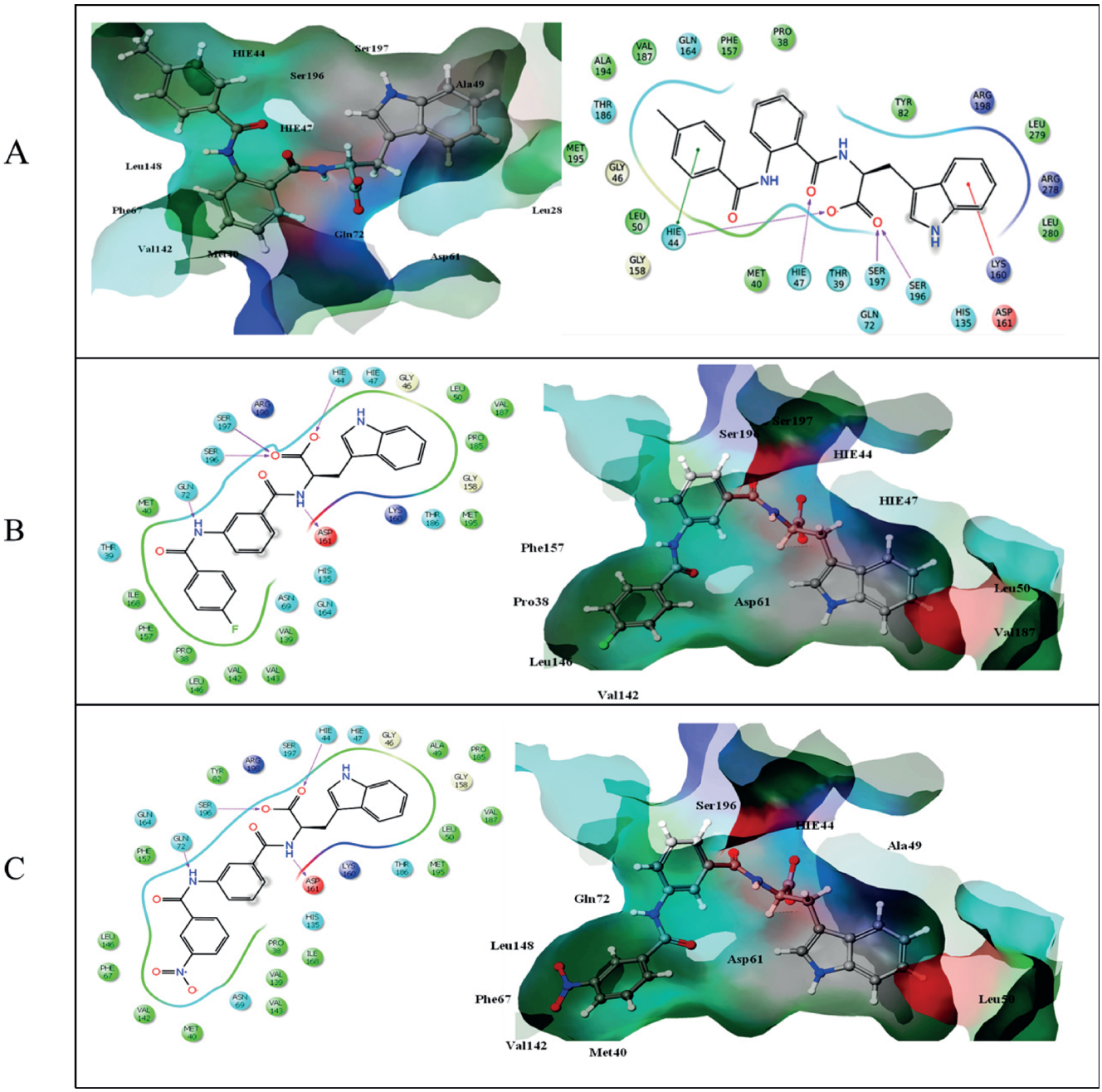

Figure 7. A. Binding pose of parent molecule (Lead 10) and its ligand interaction diagram towards the active site of the protein; B. Ligand interaction diagram and binding pose of the molecule (**5e**) and C. Ligand interaction diagram and binding pose of the molecule (**5l**).

against log phase culture of *M. tuberculosis* H37Rv by MABA assay method for the determination of minimum inhibitory concentration (MIC) in duplicates. MICs of the designed and synthesized compounds along with the standard drugs for comparison were reported in Tables 4 and 5. The comparison of designed and synthesized compounds was done with standard first line antitubercular drug isoniazid (0.72 μM) and ethambutol (7.64 μM) as positive controls. Compounds were also tested for in vitro cytotoxicity against HEK293 cell lines at 50 μM concentration using MTT assay. Percentage inhibition of cells was reported in Tables 4 and 5. None of the compounds except **5o** and **5p** were found to be cytotoxic at the concentration tested.

4 Conclusions

In the present study, we had successfully demonstrated virtual screening strategy to develop novel inhibitors against Mtb PS. Based on the first generation of hit identification;

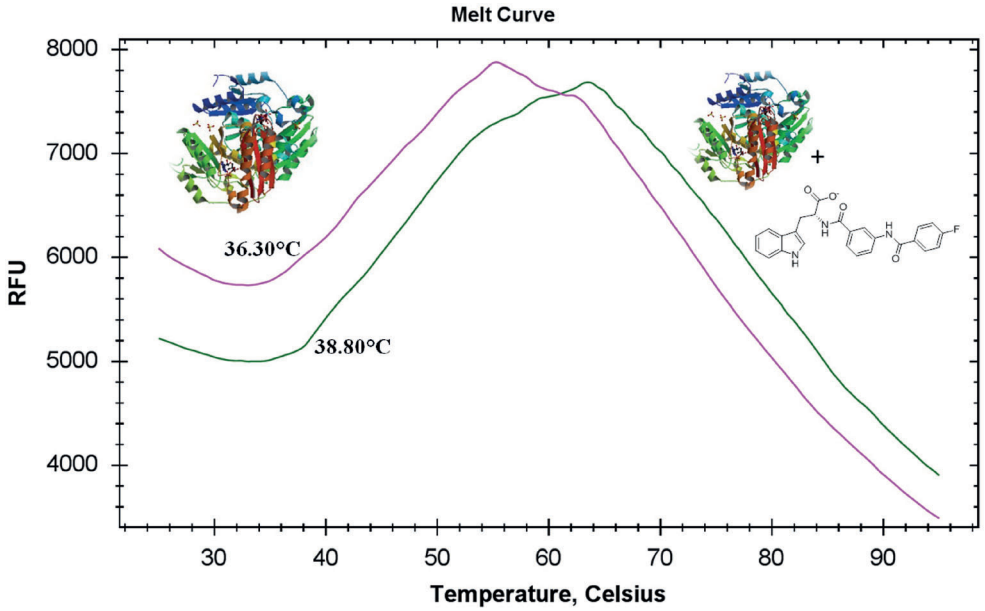

Figure 8. Thermal shift pattern for the protein (pink line) and in complex with the potent molecule **5e** (green line).

we were able to optimize the lead **10** by medicinal chemistry approach and identified a potential compound **5e** useful as inhibitor of Mtb PS. Further the compound was biophysically confirmed by differential scanning fluorimetry (DSF) to improve stability of the protein. It was satisfying to see the that **lead 10** (designed) when modified to compound **5e** (after lead optimisation) showed a positive shift in DSF, indicating an increase of thermal stability of the complex inhibitor–protein that matched the best in vitro antitubercular activity as well.

References

[1] World Health Organization (WHO), Global Tuberculosis Control **2013** report www.who.int/tb/publications/global_report/en/
[2] World Health Organization (WHO), Global Tuberculosis Control **2013** report www.who.int/tb/challenges/mdr/bedaquiline/en/
[3] *Multi-drug Resistant Tuberculosis – The Critical Challenge of Drug Resistance*, www.sirturo.com/multidrug-resistant-tb
[4] K. Takayama, C. Wang, G. S. Besra, *Clin. Microbiol. Rev.* **2005**, *18*, 81–101.
[5] L. Williams, R. Zheng, J. S. Blanchard, F. M. Raushel, *Biochemistry* **2003**, 12904–12912.
[6] V. K. Sambandamurthy, X. Wang, B. Chen, R. G. Russell, S. Derrick, F. M. Collins, S. L. Morris, W. R. Jacobs, *Nat. Med.* **2002**, *8*, 1172–1173.
[7] C. W. Murray, D. C. Rees, *Nature Chem.* **2009**, *1*, 187–192.
[8] P. J. Hajduk, J. Greer, *Nature Rev. Drug Discov.* **2007**, *6*, 211–219.
[9] G. Samala, P. B. Devi, R. Nallangi, P. Yogeeswari, D. Sriram, *Eur. J. Med. Chem.* **2013**, *69*, 356–364.
[10] G. Samala, R. Nallangi, P. B. Devi, S. Saxena, R. Yadav, J. P. Sridevi, P. Yogeeswari, D. Sriram, *Bioorg. Med. Chem.* **2014**, *22*, 4223–4232.
[11] G. Samala, P. B. Devi, R. Nallangi, J. P. Sridevi, S. Saxena, P. Yogeeswari, D. Sriram, *Bioorg. Med. Chem.* **2014**, *22*, 1938–1947.
[12] P. B. Devi, G. Samala, J. P. Sridevi, S. Saxena, A. Mallika, E. G. Salina, D. Sriram, P. Yogeeswari, *ChemMedChem* **2014**, DOI: 10.1002/cmdc.201402171R1, in press.
[13] *Maestro*, Version 9.3, Schrodinger, LLC, New York, NY, **2012**.
[14] A. W. Hung, H. L. Silvestre, S. Wen, A. Ciulli, T. L. Blundell, C. Abell, *Angew. Chem. Int. Ed. Engl.* **2009**, *48*, 8452–8456.
[15] S. L. Dixon, A. M. Smondyrev, S. N. Rao, *Chem. Biol. Drug. Des.* **2006**, *67*, 370–372.
[16] N. K. Salam, R. Nuti, W. Sherman, *J. Chem. Inf. Model.* **2009**, *49*, 2356–2368.
[17] S. Nagamani, C. Kesavan, K. Muthsam, *Bioinformation.* **2012**, *15*, 705–710.
[18] M. B. Battu, A. M. Chandra, D. Sriram, P. Yogeeswari, *Curr. Med. Chem.* **2014**, *21*, 1910–1921.
[19] S. Saxena, P. B. Devi, V. Soni, P. Yogeeswari, D. Sriram, *J. Mol. Graph. Model.* **2014**, *47*, 37–43.
[20] P. J. Therasa, D. Manvar, S. Kondepudi, M. B. Battu, D. Sriram, A. Basu, P. Yogeeswari, N. K. Basu, *J. Chem. Inf. Model.* **2014**, *54*, 539–552.
[21] E. Lucile, S. Kristen, R. Larry, C. Sara, B. Rachel, I. S. Melinda, M. Anna, R. Lynn, G. Celia, E. David, M. Thomas, *J. Biomol. Screen.* **2006**, *12*, 100–102.
[22] B. Leonard, J. Coronel, M. Siedner, L. Grandjean, L. Caviedes, P. Navarro, R. H. Gilman, D. A. J. Moore , *Clin. Microbiol.* **2008**, *46*, 3526–3528.
[23] D. Gerlier, N. Thomasset, *Immunol. Meth.* **1986**, 94, 57–63.
[24] D. A. Scudiero, R. H. Shoemaker, K. D. Paull, A. Monks, S. Tierney, T. H. Nofziger, M. J. Currens, D. Seniff, M. R. Boyd, *Cancer Res.* **1988**, *48*, 4827–4828.
[25] F. H. Niesen, H. Berglund, M. Vedadi, *Nature Prot.* **2007**, *2*, 2212–2221.

Received: September 2, 2014
Accepted: November 19, 2014
Published online: ■■ ▮▮, 0000

FULL PAPERS

*P. B. Devi, S. Jogula, A. P. Reddy, S. Saxena, J. P. Sridevi, D. Sriram, P. Yogeeswari**

■■ – ■■

Design of Novel *Mycobacterium tuberculosis* Pantothenate Synthetase Inhibitors: Virtual Screening, Synthesis and In Vitro Biological Activities